Molecular Plant Pathology

MOLECULAR PLANT PATHOLOGY (2017) 18(7), 949–962 DOI: 10.1111/mpp.12451

Xanthoferrin, the α-hydroxycarboxylate-type siderophore of *Xanthomonas campestris* pv. *campestris*, is required for optimum virulence and growth inside cabbage

SHEO SHANKAR PANDEY[1,2], PRADEEP KUMAR PATNANA[1], RIKKY RAI[1,2] AND SUBHADEEP CHATTERJEE[1,*]

[1]*Centre for DNA Fingerprinting and Diagnostics, Nampally, Hyderabad 500001, India*
[2]*Graduate Studies, Manipal University, Manipal 576104, India*

SUMMARY

Xanthomonas campestris pv. *campestris* causes black rot, a serious disease of crucifers. Xanthomonads encode a siderophore biosynthesis and uptake gene cluster *xss* (*Xanthomonas* siderophore synthesis) involved in the production of a vibrioferrin-type siderophore. However, little is known about the role of the siderophore in the iron uptake and virulence of *X. campestris* pv. *campestris*. In this study, we show that *X. campestris* pv. *campestris* produces an α-hydroxycarboxylate-type siderophore (named xanthoferrin), which is required for growth under low-iron conditions and for optimum virulence. A mutation in the siderophore synthesis *xssA* gene causes deficiency in siderophore production and growth under low-iron conditions. In contrast, the siderophore utilization Δ*xsuA* mutant is able to produce siderophore, but exhibits a defect in the utilization of the siderophore–iron complex. Our radiolabelled iron uptake studies confirm that the Δ*xssA* and Δ*xsuA* mutants exhibit defects in ferric iron (Fe^{3+}) uptake. The Δ*xssA* mutant is able to utilize and transport the exogenous xanthoferrin–Fe^{3+} complex; in contrast, the siderophore utilization or uptake mutant Δ*xsuA* exhibits defects in siderophore uptake. Expression analysis of the *xss* operon using a chromosomal *gusA* fusion indicates that the *xss* operon is expressed during *in planta* growth and under low-iron conditions. Furthermore, exogenous iron supplementation in cabbage leaves rescues the *in planta* growth deficiency of Δ*xssA* and Δ*xsuA* mutants. Our study reveals that the siderophore xanthoferrin is an important virulence factor of *X. campestris* pv. *campestris* which promotes *in planta* growth by the sequestration of Fe^{3+}.

Keywords: cabbage, ferric iron uptake, siderophore, vibrioferrin, virulence, xanthoferrin.

*Correspondence: Email: subhadeep@cdfd.org.in

INTRODUCTION

Iron uptake and metabolism are crucial for the growth and survival of bacterial pathogens inside their hosts (Cassat and Skaar, 2013; Expert *et al.*, 2012; Expert *et al.*, 1996; Guerinot, 1994). Iron acquisition by both animal- and plant-pathogenic bacteria inside their hosts acts as a crucial virulence-determining factor in many infection processes in which iron is sequestered by the host proteins (Expert *et al.*, 1996; Schaible and Kaufmann, 2004; Weinberg, 2009). Under low-iron conditions, bacteria produce and secrete siderophores (high-affinity, iron-binding compounds), which chelate ferric iron (Fe^{3+}) from the environment and facilitate its uptake (Andrews *et al.*, 2003; Neilands, 1981). The transport of the Fe^{3+}–siderophore complex occurs across the outer membrane through TonB-dependent transporters (TBDTs), which are bacterial outer membrane β-barrel proteins with 22 antiparallel β-strands (Noinaj *et al.*, 2010). Fe^{3+}–siderophore-bound outer membrane TonB-dependent transporters couple with the cytoplasmic membrane through the protein complex TonB–ExbB–ExbD, which provides the proton motive force-derived energy required for the conformational change of TBDTs to release the Fe^{3+}–siderophore complex into the periplasm (Ferguson and Deisenhofer, 2004; Larsen *et al.*, 1999; Wiener, 2005; Wiggerich *et al.*, 1997). An ABC transporter, which is a cytoplasmic-ATPase-attached transmembrane permease, delivers periplasmic Fe^{3+}–siderophores to the cytoplasm and eventually Fe^{3+} reduction occurs to release ferrous iron (Fe^{2+}) (Braun and Hantke, 2013; Faraldo-Gómez and Sansom, 2003; Krewulak and Vogel, 2008; Noinaj *et al.*, 2010).

Siderophores exhibit substantial structural diversity and can be classified into five major groups based on the moiety involved in iron coordination: catecholates (e.g. enterobactin from enteric bacteria, *Streptomyces* spp.), hydroxamates (e.g. alcaligin from *Alcaligenes denitrificans*), phenolates (e.g. yersiniabactin from *Yersinia pestis*), carboxylates (e.g. staphyloferrin from *Staphylococcus* spp.) and mixed type (e.g. aerobactin from *Enterobacter* spp.) (Miethke and Marahiel, 2007).

Earlier studies have demonstrated the requirement of siderophores in the virulence of several animal-pathogenic bacteria, such as staphyloferrin B in *Staphylococcus aureus* (Dale *et al.*,

2004), yersiniabactin in *Yersinia pestis* and *Klebsiella pneumoniae* (Bearden *et al.*, 1997; Lawlor *et al.*, 2007), pyoverdine in *Pseudomonas aeruginosa* (Meyer *et al.*, 1996) and vibriobactin in *Vibrio cholerae* (Henderson and Payne, 1994).

However, there are considerable differences in the contributions of siderophores to the virulence of plant-pathogenic bacteria. The plant-pathogenic bacterium *Erwinia chrysanthemi* 3937 synthesizes two types of siderophore, chrysobactin and achromobactin, which are required for the development of soft rot disease in African violets (*Saintpaulia ionantha*) (Enard *et al.*, 1988; Franza *et al.*, 2005). The fire blight-causing bacterium *Erwinia amylovora* produces the siderophore desferrioxamine, which is crucial for its effective infection on apple (*Malus domestica*) (Dellagi *et al.*, 1998). In contrast, siderophore-deficient mutants of *Agrobacterium tumefaciens* (Rondon *et al.*, 2004), *Ralstonia solanacearum* (Bhatt and Denny, 2004), *Erwinia carotovora* ssp. *carotovora* (Bull *et al.*, 1996) and *Pseudomonas syringae* pv. *tomato* DC3000 (Jones and Wildermuth, 2011) are virulence proficient.

Xanthomonads encode an *xss* (*Xanthomonas s*iderophore *s*ynthesis) operon which is homologous to the *Vibrio parahaemolyticus* siderophore (*pvs*) locus and produces a vibrioferrin-type siderophore under iron-restricted conditions (Pandey and Sonti, 2010; Rai *et al.*, 2015). In *Xanthomonas oryzae* pv. *oryzae* (Xoo; a vascular pathogen of rice), it has been shown that siderophore production is not required for virulence in rice (Pandey and Sonti, 2010). Interestingly, the Xoo *xss* cluster is induced under low-iron conditions; however, it is not expressed *in planta* (Pandey and Sonti, 2010).

In *Xanthomonas campestris* pv. *campestris* (Xcc), the TonB-dependent Fe^{3+} acquisition system (*exbB*, *exbD1* and *exbD2*) has been proposed to play a role in virulence. However, the role of the siderophore in iron uptake and virulence has not been demonstrated clearly in this bacterium (Wiggerich and Pühler, 2000). In order to understand the role of the siderophore in Xcc virulence and iron uptake, we characterized the siderophore biosynthesis (*xssA*) and utilization (*xsu*A) mutants of Xcc 8004. In this study, we show that Xcc produces xanthoferrin, which is similar to the α-hydroxycarboxylate-type siderophore vibrioferrin. We demonstrate that the production and utilization of xanthoferrin are required for Xcc growth under low-iron conditions and contribute to its virulence and growth inside its cabbage host.

RESULTS

Δ*xssA* mutant of Xcc is deficient in xanthoferrin production

The genome of strain Xcc 8004 (Qian *et al.*, 2005) possesses a homologue of the *Xanthomonas* siderophore synthesis and utilization locus similar to the Xoo *xss* and *V. parahaemolyticus pvs* locus (Fig. S1; Table S1, see Supporting Information; Pandey and Sonti, 2010; Tanabe *et al.*, 1982). The *xssA* (XC_1107) gene product from the Xcc 8004 strain exhibits high homology to XssA from Xoo (identity 86%, similarity 90%) and PvsA from *V. parahaemolyticus* (identity 46%, similarity 64%). The siderophore utilization gene product *xsu*A exhibits high homology to XsuA from Xoo (identity 87%, similarity 92%) and PvuA from *V. parahaemolyticus* (identity 45%, similarity 61%) (Table S1).

In order to understand the role of the siderophore in Xcc virulence, we constructed in-frame marker-free deletions of *xssA* (XC_1107) and *xsuA* (XC_1108) genes in the wild-type Xcc 8004 strain (see Experimental Procedures; Fig. S2A; Table S2, see Supporting Information). Expression analysis by quantitative reverse transcription-polymerase chain reaction (qRT-PCR) indicated that the expression of downstream genes is not altered in the deletion mutants relative to the wild-type strain (Fig. S3, see Supporting Information). This result suggests that the in-frame deletion of *xssA* and *xsuA* genes does not have a possible polar effect on the expression of genes located downstream. The ability of these mutants to produce siderophores was assessed on peptone–sucrose agar and chromeazurol S (PSA–CAS) medium containing 75 μM 2,2′-dipyridyl (DP; specific Fe^{2+} chelator). In contrast with the wild-type Xcc 8004 strain, the Δ*xssA* mutant failed to produce a halo on PSA–CAS–DP medium (Fig. 1A). Complementation of the Δ*xssA* mutant with a plasmid harbouring the entire *xss* cluster from Xoo (pAP15; Pandey and Sonti, 2010; Table S2) rescued the siderophore production defect.

We isolated siderophores from the cell-free culture supernatant of wild-type Xcc 8004, Δ*xssA*, Δ*xsuA*, and mutants harbouring the complementing plasmid pAP15 (Δ*xssA*/pAP15 and Δ*xsuA*/pAP15) with Amberlite XAD-16 resin columns (see Experimental Procedures) and checked for activity on PSA–CAS–DP plates (Fig. 1A). The siderophore was further purified from active fractions by high-performance liquid chromatography (HPLC) and compared with the elution profile of the purified α-hydroxycarboxylate-type siderophore vibrioferrin (Fujita *et al.*, 2011). The HPLC analysis indicated that the fractions corresponding to the purified active Xcc siderophore and standard synthetic vibrioferrin exhibited similar retention times (Fig. S4, see Supporting Information). We named the purified active siderophore from the Xcc 8004 strain as 'xanthoferrin', which is similar to vibrioferrin produced by *V. parahaemolyticus* and *V. alginolyticus* (Fujita *et al.*, 2011; Pandey and Sonti, 2010; Rai *et al.*, 2015; Tanabe *et al.*, 1982). The concentration of xanthoferrin produced by different strains of Xcc was determined on the basis of the peak area and calculated from standard curves generated from known concentrations of standard vibrioferrin by HPLC analysis (Fujita *et al.*, 2011). The wild-type Xcc 8004 strain produced approximately 12 μg of xanthoferrin per 10^9 cells (Fig. 1B). In contrast, the Δ*xssA* mutant produced a negligible amount of xanthoferrin siderophore, which could be complemented by the plasmid harbouring the *xss* cluster from

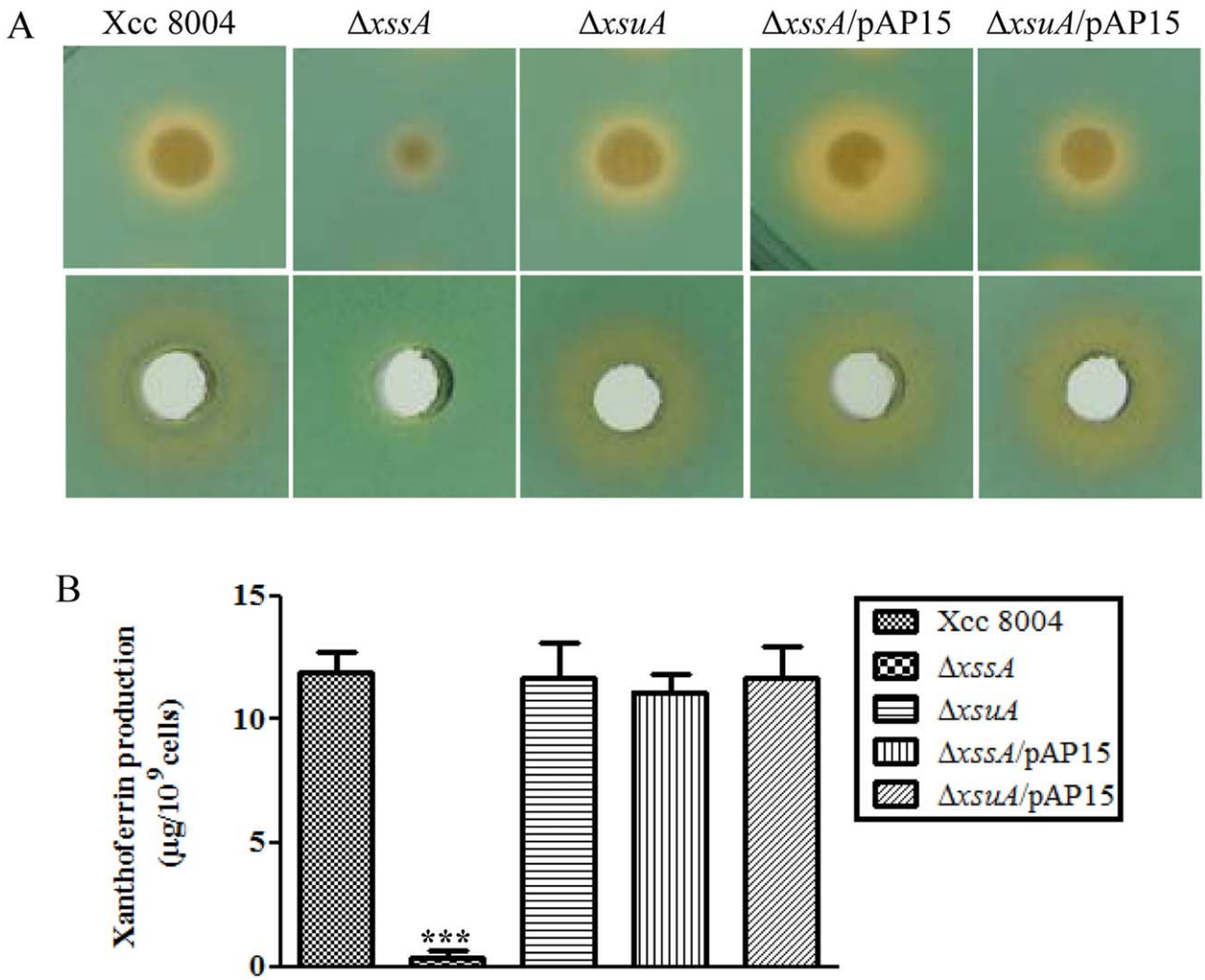

Fig. 1 *xssA* gene is required for siderophore xanthoferrin biosynthesis in *Xanthomonas campestris* pv. *campestris* (Xcc). (A) Top: siderophore production by different Xcc strains on peptone–sucrose agar and chromeazurol S (PSA–CAS) plates containing 75 μM of the ferrous iron chelator 2,2′-dipyridyl. Strains: Xcc 8004 (wild-type strain); Δ*xssA* [deletion of *xssA* (*Xanthomonas s*iderophore *s*ynthesis A)]; Δ*xsuA* [deletion of *xsuA* (*Xanthomonas s*iderophore *u*ptake A)]; Δ*xssA*/pAP15; and Δ*xsuA*/pAP15 (pAP15; wild-type *xssA* and *xsuA* alleles). Bottom: wells on PSA–CAS plate containing siderophore isolated from the cell-free culture supernatant of different strains of Xcc grown under low-iron conditions [peptone–sucrose (PS) + 100 μM 2,2′-dipyridyl] using Amberlite XAD-16 resin column chromatography. Cell-normalized siderophore fractions were loaded into wells prepared on a PSA–CAS indicator plate (with 75 μM 2,2′-dipyridyl). (B) Quantification of purified xanthoferrin of different Xcc strains. Strains were grown to late exponential phase in low-iron medium (PS + 100 μM 2,2′-dipyridyl). Siderophores were initially purified from cell-free culture supernatants using Amberlite XAD-16 resin columns. The cell-normalized active fraction of siderophore was analysed by high-performance liquid chromatography (HPLC). Xanthoferrin was detected at 300 nm. The amount of xanthoferrin was determined by comparing the peak area (mAU × min) with the standard curve which was generated from a known concentration of pure standard vibrioferrin.

Xoo (Figs 1B and S4). However, the siderophore utilization Δ*xsuA* mutant did not exhibit any defect in xanthoferrin production (Figs 1B and S4).

Xanthoferrin-mediated iron uptake is required for growth under low-iron conditions

To understand the role of xanthoferrin during growth under low-iron conditions, we compared the growth profile of wild-type Xcc 8004, Δ*xssA*, Δ*xsuA*, Δ*xssA*/pAP15 and Δ*xsuA*/pAP15 strains in peptone–sucrose (PS) (rich medium), PS–DP (low-iron conditions; PS medium containing 150 μM DP) and PS–DP medium supplemented with either purified xanthoferrin siderophore or Fe^{2+} sulfate (Fig. 2). The growth patterns of wild-type and mutants were indistinguishable in rich medium (doubling time of approximately 2.8 h; Fig. 2A; Table 1). Under low-iron conditions (PS–DP), the doubling time of the wild-type Xcc 8004 strain was 3.9 h. However, the doubling times of Δ*xssA* and Δ*xsuA* mutants were

significantly less (doubling time of 5.5 h) than that of the wild-type strain (Fig. 2B; Table 1) grown under low-iron conditions. The growth defect exhibited by the Δ*xssA* and Δ*xsuA* mutants under low-iron conditions could be rescued by complementation with the plasmid harbouring the Xoo *xss* gene cluster (Fig. 2A,B; Table 1). Interestingly, supplementation of purified xanthoferrin siderophore could rescue the growth defect of Δ*xssA* (doubling time of approximately 4 h), but failed to restore the growth defect exhibited by Δ*xsuA* in low-iron medium (doubling time 5.9 h) (Fig. 2C; Table 1). Furthermore, supplementation of purified vibrioferrin from *V. parahaemolyticus* also rescued the growth defect of the Δ*xssA* mutant, similar to xanthoferrin supplementation (Fig. S5; Table S3, see Supporting Information).

Δ*xssA* and Δ*xsuA* mutants exhibit less intracellular iron content under low-iron conditions

The bactericidal activity of the quinone antibiotic streptonigrin is strongly dependent on the formation of oxygen radicals, which has a direct correlation with the availability of intracellular iron in bacteria. The hypersensitivity of bacterial cells towards streptonigrin indicates a higher intracellular level of iron (Cohen *et al.*, 1987; Schmitt, 1997; Yeowell and White, 1982). Therefore, to assess the intracellular iron content of different Xcc strains, we performed streptonigrin sensitivity assay in rich PS, low-iron and iron-replete media (Figs 3A and S6, see Supporting Information). We observed that Δ*xssA* and Δ*xsuA* mutants exhibited a 35%–40% increase in survival rate compared with the wild-type strain after 16 and 42 h of growth under low-iron conditions in the presence of streptonigrin. This result suggests that the Δ*xssA* and Δ*xsuA* mutants hold less intracellular iron in the low-iron medium relative to the wild-type Xcc 8004, a phenotype which can be restored by complementation *in trans* (Fig. 3A). In rich (PS) and iron-replete (PS + 100 μM $FeSO_4$) media, there was no significant difference observed in the survival rate of these mutants relative to the wild-type Xcc 8004 (Fig. S6A–D). Further, we performed atomic absorption spectroscopy to measure directly intracellular elemental iron in different Xcc strains. Iron estimation by inductively coupled plasma-optical emission spectrometry (ICP-OES) further indicated approximately two-fold less intracellular iron content in the Δ*xssA* and Δ*xsuA* mutants under low-iron conditions, which was restored by *in trans* expression of the wild-type Xoo *xss* gene cluster in the mutant background (Fig. 3B). However, we did not observe any significant difference in the intracellular iron content of Δ*xssA* and Δ*xsuA* mutants relative to the wild-type Xcc 8004 strain in either rich PS medium or iron-replete conditions (PS + 100 μM $FeSO_4$) (Fig. S6E,F).

Expression of the *xss* operon is induced under low-iron conditions and during *in planta* growth

To investigate the role of xanthoferrin during the *in planta* growth of Xcc, we performed expression analysis inside the plant using a chromosomal fusion of the upstream putative promoter of the *xss* cluster with the β-glucuronidase (*gusA*) reporter gene in the wild-type Xcc 8004 background (Fig. S2; Table S2). The Xcc 8004 P*xss*::*gusA* reporter strain exhibited phenotypes similar to the wild-type Xcc strain when grown under low-iron conditions (Fig. S7, see Supporting Information). Cabbage leaves were infiltrated with the Xcc 8004 P*xss*::*gusA* strain with and without $FeSO_4$ or DP. GUS activity was monitored by staining the leaves with the chromogenic substrate X-Gluc (5-bromo-4-chloro-3-indolyl-β-D-glucuronide; see Experimental Procedures). The histochemical blue–green GUS staining was detected in leaves inoculated with the Xcc 8004 P*xss*::*gusA* reporter strain at 5 days post-inoculation (dpi). Leaves co-infiltrated with DP and Xcc 8004 P*xss*::*gusA* reporter strain exhibited slightly more intense GUS staining relative to leaves infiltrated with the Xcc 8004 P*xss*::*gusA* strain alone (Fig. 4A). The intensity of GUS staining decreased strongly in leaves co-infiltrated with Xcc 8004 P*xss*::*gusA* strain with Fe^{2+} (Fig. 4A). GUS activity was measured from the extracts of cabbage leaves inoculated with the Xcc 8004 P*xss*::*gusA* reporter strain from 0 to 8 dpi. GUS assay indicated significant *in planta* expression of the *xss* operon (Fig. 4B). There was approximately 100-fold decrease in GUS activity in leaves co-infiltrated with Xcc 8004 P*xss*::*gusA* and iron compared with those infiltrated with Xcc 8004 P*xss*::*gusA* strain alone. In addition, we performed *in vitro* expression analysis with the chromosomal fusion of P*xss*::*gusA* grown in rich (PS), low-iron (PS + DP) and low-iron medium supplemented with Fe^{2+}. There was approximately three- to four-fold induction in the expression of the *xss* gene cluster under low-iron conditions relative to rich PS medium. The addition of exogenous iron to the low-iron medium suppressed the expression of the *xss* operon (Fig. 4C).

Δ*xssA* and Δ*xsuA* mutants are defective in Fe^{3+} uptake and exogenous xanthoferrin restores Fe^{3+} uptake in Δ*xssA*

To understand the contribution of xanthoferrin in iron uptake, we performed *in vitro* iron uptake assay to measure the iron transport ability of wild-type Xcc 8004, Δ*xssA*, Δ*xsuA* and the mutants harbouring the wild-type Xoo *xss* cluster (pAP15) using radiolabelled iron, as described previously (Ardon *et al.*, 1997; Velayudhan *et al.*, 2000) with a few modifications (see Experimental Procedures). The total amounts of radiolabelled Fe^{3+} incorporated into the Δ*xssA* and Δ*xsuA* mutants were significantly less (approximately two-fold lower) than in the wild-type Xcc 8004, Δ*xssA*/pAP15 and Δ*xsuA*/pAP15 over the 10-min time course of the uptake assay experiment (Fig. 5A). In addition, we performed the Fe^{3+} uptake assay with the Fe^{3+}–xanthoferrin complex. The

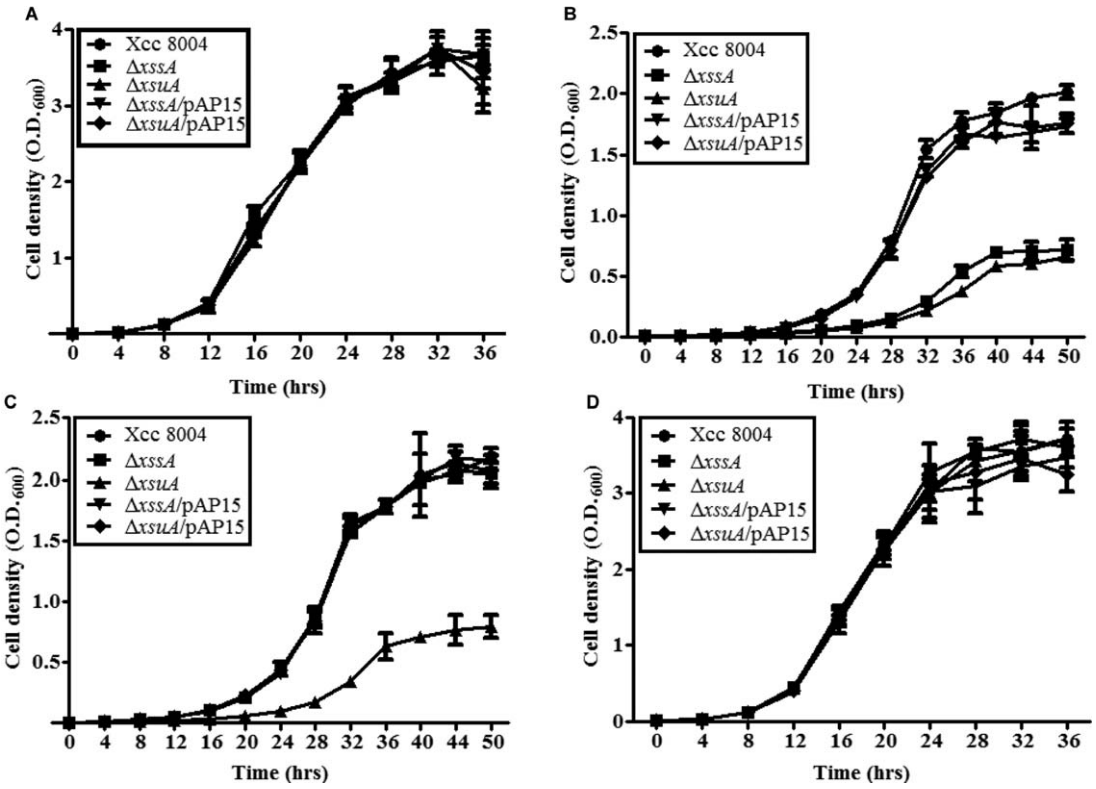

Fig. 2 The Δ*xssA* and Δ*xsuA* mutants are growth deficient under low-iron conditions. Growth of *Xanthomonas campestris* pv. *campestris* (Xcc) 8004, Δ*xssA*, Δ*xsuA*, Δ*xssA*/pAP15 and Δ*xsuA*/pAP15 strains under the following conditions: (A) rich peptone–sucrose (PS) medium; (B) low-iron medium (PS + 150 μM intracellular ferrous iron chelator 2,2′-bipyridyl); (C) xanthoferrin-supplemented low-iron medium (PS + 150 μM 2,2′-dipyridyl + 20 μm xanthoferrin); (D) ferrous iron-supplemented low-iron medium (PS + 150 μM 2,2′-dipyridyl + 100 μM $FeSO_4$). Growth was monitored by determination of the optical density at 600 nm (OD_{600}). Data are shown as mean ± standard deviation (SD) ($n = 3$).

xanthoferrin-mediated incorporation of radiolabelled Fe^{3+} was of a similar level in Δ*xssA* and wild-type Xcc 8004, but the Δ*xsuA* mutant was defective in xanthoferrin-mediated Fe^{3+} uptake (Fig. 5B). However, we did not observe any significant difference in radiolabelled Fe^{2+} uptake in the Δ*xssA* and Δ*xsuA* mutants compared with the wild-type Xcc 8004 (data not shown).

Xanthoferrin synthesis and uptake are required for the optimum virulence of Xcc 8004 on cabbage

To understand the role of xanthoferrin in the virulence of Xcc, we performed infection studies with wild-type Xcc 8004, Δ*xssA*, Δ*xsuA*, Δ*xssA*/pAP15 and Δ*xsuA*/pAP15 strains on cabbage plants. We inoculated cabbage leaves with bacterial cell

Table 1 Generation times of *Xanthomonas campestris* pv. *campestris* (Xcc) strains.

	Generation time (h)*			
	PS	PS + DP†	PS + DP + $FeSO_4$‡	PS + DP + xanthoferrin§
Xcc 8004	2.86 ± 0.06	3.98 ± 0.03	2.84 ± 0.13	4.19 ± 0.14
Δ*xssA*	2.85 ± 0.04	5.56 ± 0.38¶	2.82 ± 0.1	4.06 ± 0.13
Δ*xsuA*	2.85 ± 0.13	5.51 ± 0.37¶	2.85 ± 0.1	5.91 ± 0.52¶
Δ*xssA*/pAP15	2.83 ± 0.11	3.92 ± 0.19	2.8 ± 0.04	4.15 ± 0.11
Δ*xsuA*/pAP15	2.9 ± 0.04	3.89 ± 0.07	2.88 ± 0.07	4.31 ± 0.19

*Generation times are the means of three biological replicates ± standard deviation (SD).

†150 μM 2,2′-dipyridyl (DP) was added to peptone–sucrose (PS) medium to yield low-iron conditions.

‡100 μM of $FeSO_4$ was added to supplement the low-iron medium.

§20 μM of xanthoferrin was added to supplement the low-iron medium.

¶$P < 0.01$ vs. wild-type in the same medium by two-tailed paired Student's *t*-test.

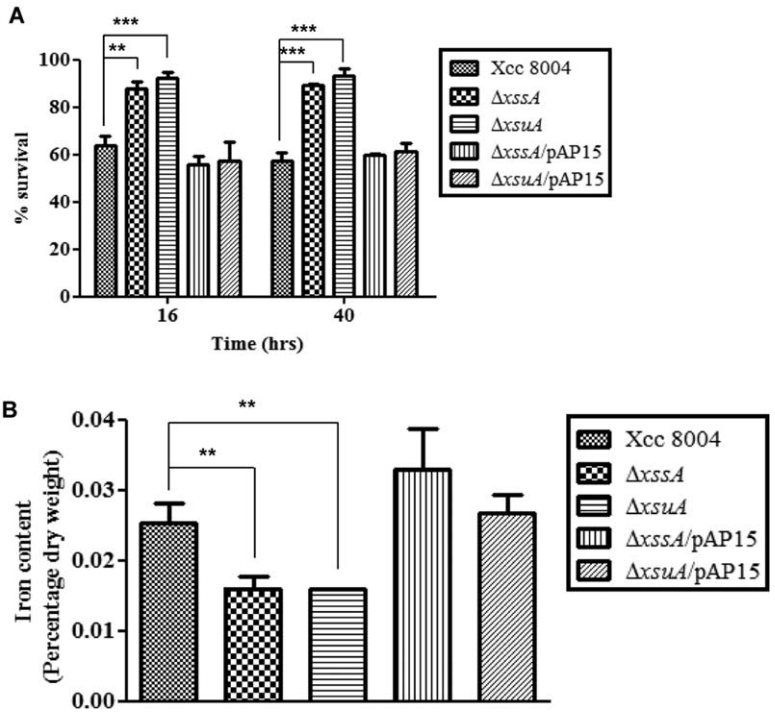

Fig. 3 The Δ*xssA* and Δ*xsuA* mutants exhibit less intracellular iron content under low-iron conditions. (A) Streptonigrin (SNG) sensitivity assay in broth. Percentage survival of different *Xanthomonas campestris* pv. *campestris* (Xcc) strains in peptone–sucrose (PS) + 150 μM 2,2′-dipyridyl + 0.5 μg/mL SNG + 0.01 M sodium citrate after 16 and 42 h of growth. Percentage survival in SNG was calculated by comparison with growth in PS + 150 μM 2,2′-dipyridyl as described in Experimental Procedures. (B) Intracellular iron content quantification determined by inductively coupled plasma-optical emission spectrometry (ICP-OES). Different Xcc strains were grown to late exponential phase in low-iron medium (PS + 150 μM intracellular ferrous iron chelator 2,2′-dipyridyl). Cells were harvested by centrifugation, freeze dried and solubilized in 30% HNO_3 as described in Experimental Procedures. The data shown in the graphs are the mean ± standard error (SE) ($n = 3$). $^{**}P < 0.01$; $^{***}P < 0.001$; statistical significance by paired Student's *t*-test.

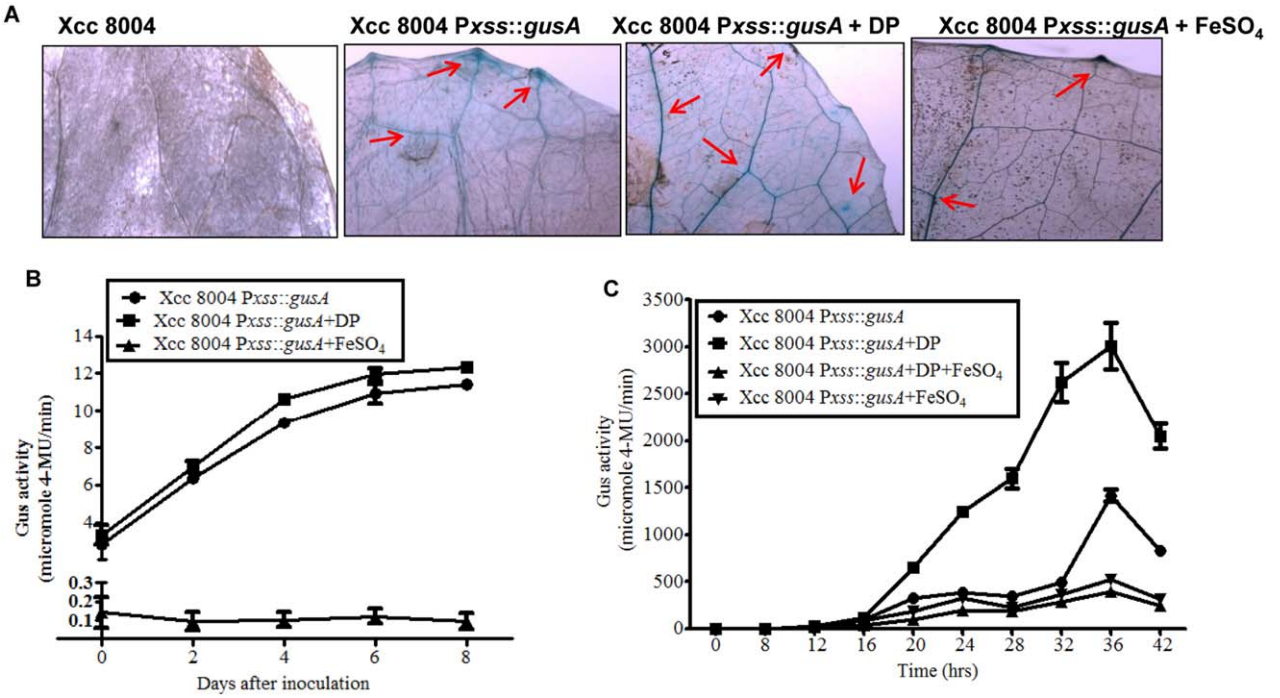

Fig. 4 The *xss* (*Xanthomonas* siderophore synthesis) gene cluster is expressed during the *in planta* growth of *Xanthomonas campestris* pv. *campestris* (Xcc). (A) Histochemical β-glucuronidase (GUS) staining with the chromogenic substrate X-Gluc (5-bromo-4-chloro-3-indolyl-β-D-glucuronide) of cabbage leaves infiltrated with reporter strain Xcc 8004 P*xss::gusA* with water, 100 μM 2,2′-dipyridyl or 200 μM $FeSO_4$. Control is a GUS-negative Xcc 8004 strain. Arrows indicate GUS staining in veins. (B) *In planta* expression analysis of *xss* gene cluster in wild-type (Xcc 8004 P*xss::gusA*). GUS activity was monitored from 1 cm^2 of cabbage leaves inoculated with reporter strain Xcc 8004 P*xss::gusA* with water, 100 μM 2,2′-dipyridyl or 200 μM $FeSO_4$. (C) Cell-normalized *in vitro* GUS assay of reporter strain Xcc 8004 P*xss::gusA* in rich peptone–sucrose (PS), low-iron (PS + 150 μM 2,2′-dipyridyl), iron-supplemented low-iron (PS + 150 μM 2,2′-dipyridyl + 100 μM $FeSO_4$) and excess iron (PS + 100 μM $FeSO_4$) media. 4-MU, 4-methylumbelliferone.

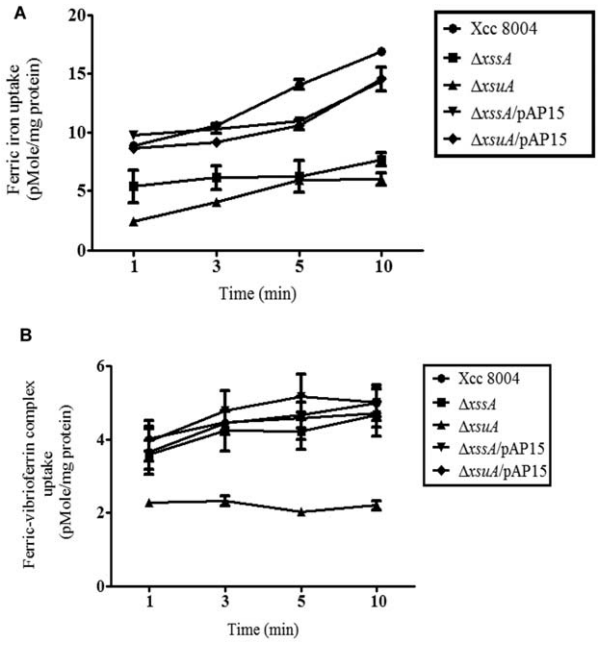

Fig. 5 The Δ*xssA* and Δ*xsuA* mutants are defective in ferric iron uptake and xanthoferrin supplementation restores ferric iron uptake in the Δ*xssA* mutant. (A) The Δ*xssA* and Δ*xsuA* mutants show deficiency in ferric iron uptake under low-iron conditions. The ferric iron transport was initiated by the addition of 0.4 μM $^{55}FeCl_3$ to cell suspensions of wild-type Xcc 8004, Δ*xssA*, Δ*xsuA*, Δ*xssA*/pAP15 and Δ*xsuA*//pAP15 strains. (B) Xanthoferrin supplementation restores the ferric iron uptake deficiency of Δ*xssA*. The ferric-xanthoferrin complex transport was initiated by the addition of 0.4 μM 1 : 1 ratios of $^{55}FeCl_3$ and xanthoferrin to cell suspensions of various *Xanthomonas campestris* pv. *campestris* (Xcc) strains grown under low-iron conditions. Data are shown as mean ± standard error (SE) ($n = 3$).

suspensions by the leaf clip method and monitored lesion development, bacterial migration inside the leaves and *in planta* bacterial growth (see Experimental Procedures; Fig. S8, see Supporting Information). The Δ*xssA* and Δ*xsuA* mutants were significantly compromised in lesion development, which was rescued by plasmid harbouring the Xoo *xss* cluster (pAP15) (Fig. 6A,B). The lesions caused by the wild-type Xcc 8004 strain were approximately 3 cm in length at 21 dpi. In contrast, the lesions caused by Δ*xssA* and Δ*xsuA* mutants were approximately 1 cm in length at 21 dpi (Fig. 6B). To monitor bacterial migration inside cabbage leaves, surface-sterilized infected leaves (5 dpi) were cut into 1-cm pieces from the bottom of the leaf to the top (site of inoculation) with sterile scissors, and were incubated on PSA medium containing appropriate antibiotics (Fig. S8A). Migration was estimated by observing the colonies formed after 1–3 days by bacterial ooze from the cut ends of the cabbage leaf pieces. Migration assay indicated that the Δ*xssA* and Δ*xsuA* mutants exhibited reduced *in planta* migration relative to the wild-type Xcc 8004 strain (Fig. 6C). *In planta* growth assay (0–14 dpi) indicated that the Δ*xssA* and Δ*xsuA* mutants exhibited significantly reduced growth (approximately four-fold less) than that exhibited by the wild-type Xcc 8004 strain or the mutants harbouring the complementing plasmid (Fig. 6D).

Exogenous iron supplementation promotes the growth of Δ*xssA* and Δ*xsuA* mutants in cabbage leaves

To investigate whether iron supplementation can rescue the growth defect of Δ*xssA* and Δ*xsuA* mutants inside host leaves, detached leaf assays were performed as described previously (Chatterjee and Sonti, 2002) with modifications (see Experimental Procedures; Fig. S8B). The detached cabbage leaves were maintained in beakers with or without iron (50 μM $FeCl_3$) supplementation. Benzyl amino purine (BAP), a first-generation synthetic cytokinin, was added to each beaker to maintain the freshness of the leaves. The detached cabbage leaves were inoculated with different Xcc strains and bacterial growth within the leaves was estimated at 0, 24, 48 and 72 h post-inoculation. *In planta* growth assay indicated that exogenous iron supplementation rescued the growth defect exhibited by the Δ*xssA* and Δ*xsuA* mutants (Fig. 6E). In contrast, iron supplementation in cabbage leaves did not significantly affect the growth of wild-type Xcc 8004, Δ*xssA*/pAP15 and Δ*xsuA*/pAP15 strains (Fig. 6E).

DISCUSSION

In this study, we have characterized the role of the siderophore in the virulence of Xcc, a pathogen of crucifers. The results of this study have established the following: Xcc produces xanthoferrin, an α-hydroxycarboxylate-type siderophore similar to vibrioferrin, under low-iron conditions; xanthoferrin production is required for growth under low-iron conditions and for virulence; the xanthoferrin production and uptake mutants Δ*xssA* and Δ*xsuA* exhibit defects in Fe^{3+} uptake; and exogenous supplementation of iron promotes the *in planta* growth of Δ*xssA* and Δ*xsuA* mutants in cabbage.

Xanthomonas axonopodis pv. *citri* (Xac) and Xcc possess non-ribosomal peptide synthetase (NRPS) enzymes encoding the genes Xac3922 and Xcc3867, respectively, which show similarity to enterobactin, a catecholate-type siderophore, synthase component F (EntF) in *Escherichia coli* (Etchegaray *et al.*, 2004; Ryan *et al.*, 2011; da Silva *et al.*, 2002). It has been proposed that the siderophores produced by Xac and Xcc do not belong to the catechol or hydroxamate family, but might be assigned to an unknown novel category (Etchegaray *et al.*, 2004). The genome sequence of Xcc 8004 (Qian *et al.*, 2005) indicated that it possesses an *xss* gene cluster, homologous to the Xoo *xss* locus (Lee *et al.*, 2005; Pandey and Sonti, 2010) and *V. parahaemolyticus pvs* locus (Tanabe *et al.*, 1982), which is involved in siderophore synthesis and uptake (Fig. S1). Siderophore purified from the cell-free culture supernatant by Amberlite XAD-16 resin columns and HPLC

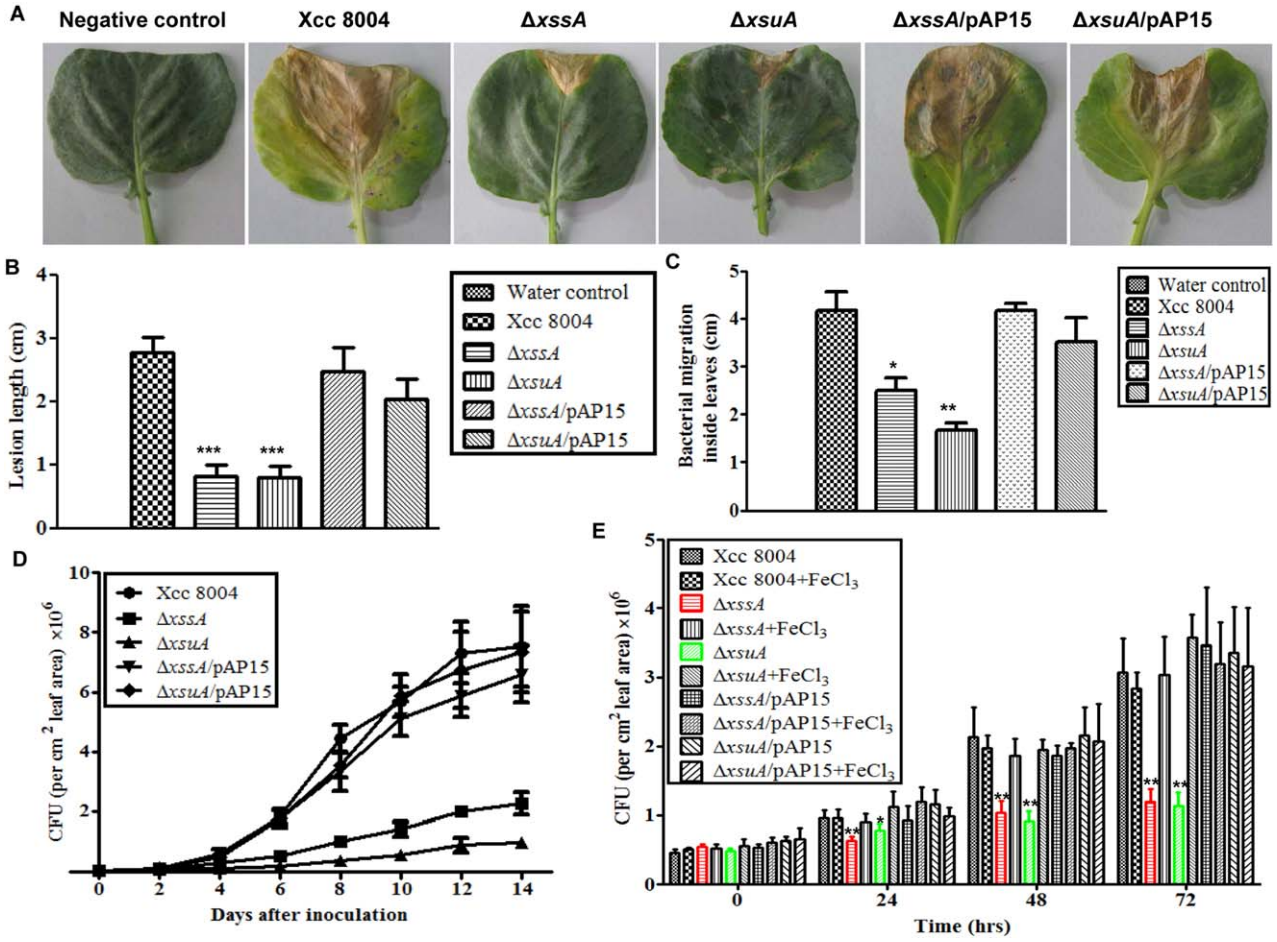

Fig. 6 The Δ*xssA* and Δ*xsuA* mutants are deficient in virulence and growth inside cabbage. (A) Cabbage leaves (Indian Super Hybrid variety) infected with wild-type Xcc 8004, Δ*xssA*, Δ*xsuA*, Δ*xssA*/pAP15 and Δ*xsuA*//pAP15 strains showing lesion symptoms at 21 days post-inoculation. Bacterial cultures (1×10^9 cells/mL suspension) were inoculated into 30-day-old plants by the clip method. (B) Quantification of lesion length at 21 days post-inoculation. Twenty-five leaves were inoculated per strain. (C) Bacterial migration at 5 days post-inoculation in host leaves was assayed by inoculating 1-cm pieces of infected leaf, cut from the base to the tip, on a peptone–sucrose agar (PSA) plate with the respective antibiotics (see Table S2). Migration was estimated by observing colonies formed after 1–3 days by bacterial ooze from the cut ends of the cabbage leaf pieces. For each experiment, six leaves were used (three independent experiments). (D) *In planta* growth assays of wild-type Xcc 8004, Δ*xssA*, Δ*xsuA*, Δ*xssA*/pAP15 and Δ*xsuA*//pAP15 strains. Bacterial populations were measured by crushing leaves (1 cm^2) followed by serial dilution plating at the indicated post-inoculation days. For each experiment, six leaves were used (three independent experiments). (E) Detached leaf assay with exogenous iron supplementation. Different Xcc strains were inoculated on detached cabbage leaves by the clip method. The leaves were maintained in 1 μg/mL of benzyl amino purine (BAP; first-generation synthetic cytokinin) with or without 50 μM $FeCl_3$ supplementation. Bacterial populations were determined from a leaf area of 1 cm^2 at the indicated post-inoculation days. The data shown in the graphs are the mean ± standard error (SE) ($n = 3$). *$P < 0.05$; **$P < 0.01$; ***$P < 0.001$; significant difference between the data obtained from mutants and the data obtained from the wild-type and complemented strains by paired Student's *t*-test. CFU, colony-forming unit.

analysis suggests that Xcc 8004 synthesizes a xanthoferrin siderophore (similar to the vibrioferrin of *V. parahaemolyticus*) under iron-limited conditions, which is an α-hydroxycarboxylate-type siderophore (Figs 1A and S4). The homology of the *xssA* gene to *pvsA*, the vibrioferrin synthesis gene of *V. parahaemolyticus*, and the drastic reduction in xanthoferrin production in the Δ*xssA* mutant suggest that *xssA* encodes a protein which is involved in xanthoferrin synthesis (Fig. 1B; Table S1). Furthermore, rescue of the growth defect exhibited by the Δ*xssA* mutant of Xcc by the exogenous supplementation of purified vibrioferrin from *V. parahaemolyticus* strongly suggests that the xanthoferrin form Xcc and vibrioferrin are structurally related (Fig. S5).

In Xoo, a xylem-specific pathogen of rice, it has been demonstrated that siderophore production is not required for virulence and the *xss* cluster is not expressed *in planta* (Pandey and Sonti, 2010). In contrast, it has been shown that, in *Xanthomonas oryzae* pv. *oryzicola* (Xoc; a pathogen of rice parenchyma), siderophore production is required for virulence and is induced *in planta*

(Rai *et al.*, 2015). These studies suggest that the contribution of the *xss* locus in pathogenicity seems to be variable among closely related xanthomonads. Our results indicate that siderophore-mediated iron uptake is required for the virulence and colonization of Xcc. We speculate that differences in host iron storage and forms (Fe^{2+} vs. Fe^{3+}) may contribute to differences in iron utilization strategies and need for closely related pathogens.

Many bacteria acquire iron through energy-independent, low-affinity iron uptake systems in iron-rich environments; however, in iron-limited environments, siderophore-mediated iron uptake occurs, which is a highly energy-dependent process (Jones and Niederweis, 2010; Noinaj *et al.*, 2010). We observed that Xcc 8004 produces siderophores under low-iron conditions, which ceases on iron supplementation (data not shown). Although, iron or xanthoferrin supplementation restores the impaired growth of the Δ*xssA* mutant under iron-limited conditions, the addition of xanthoferrin fails to restore the compromised growth of the Δ*xsuA* mutant in low-iron medium (Fig. 2C). Similarly, xanthoferrin supplementation restores the impaired Fe^{3+} uptake of the Δ*xssA* mutant, but fails to restore the Fe^{3+} uptake deficiency of the Δ*xsuA* mutant (Fig. 5B). These results suggest that *xsuA*, a homologue of *V. parahaemolyticus pvuA* (a receptor for the Fe^{3+}–siderophore complex), encodes an outer membrane receptor protein required for xanthoferrin-mediated Fe^{3+} uptake. Quantitative GUS reporter assay suggests that the expression of the *xss* operon is induced under low-iron conditions and is suppressed to the basal level after iron supplementation (Fig. 4C). The Δ*xssA* and Δ*xsuA* mutants possess less intracellular iron than the wild-type Xcc 8004 grown under iron-limited conditions (Fig. 3). These results indicate that Xcc 8004 requires xanthoferrin-mediated iron uptake, particularly in the iron-limited environment of the plant. Siderophore-independent, low-affinity iron uptake systems maintain iron homeostasis under iron-replete conditions in many microorganisms (Andrews *et al.*, 2003). The porins, Msp in *Mycobacterium smegmatis* (Jones and Niederweis, 2010) and the SFU system in *Serratia marcescens* (Angerer *et al.*, 1990; Zimmermann *et al.*, 1989), have been reported to be involved in siderophore-independent Fe^{3+} uptake. The FeoB system is involved in the uptake of the less commonly available, but soluble, Fe^{2+} form of iron (Cartron *et al.*, 2006; Kammler *et al.*, 1993). Extracellular or cell-associated Fe^{3+} reductases have been reported in many bacteria, which assist in iron uptake by increasing the availability of the soluble form of iron by reducing Fe^{3+} to Fe^{2+} (Schröder *et al.*, 2003). In our study, we detected Fe^{3+} reductase activity in Xcc strains, but no significant difference was observed among wild-type Xcc 8004, Δ*xssA* and Δ*xsuA* mutants (Fig. S9, see Supporting Information). It is pertinent to note that the iron uptake facilitated by Fe^{3+} reductases and low-affinity iron uptake systems might be sufficient to fulfil the iron requirement under rich or iron-replete conditions. However, under iron-depleted conditions, Xcc 8004 may depend particularly on xanthoferrin-mediated iron uptake. This might be the reason why the *xss* cluster is induced under iron-limiting conditions.

In planta GUS reporter assay indicated that the *xss* operon is expressed in the iron-limited host environment, but is suppressed on co-infiltration of the reporter strain and iron in cabbage leaves (Fig. 4). These results suggest that Xcc 8004 requires xanthoferrin-mediated iron uptake in the iron-limiting environment of the host. The disruption of either xanthoferrin synthesis or the xanthoferrin-mediated iron uptake system diminishes the ability of Xcc to grow, colonize and migrate inside cabbage leaves (Fig. 6). The results of the detached leaf assay suggested that the *in planta* growth deficiency of Δ*xssA* and Δ*xsuA* mutants can be rescued by the exogenous supplementation of a moderate amount of iron (Fig. 6E). Thus, there is a correlation between xanthoferrin-mediated iron uptake and the ability of Xcc to cause disease. These data suggest that the ability to acquire iron by the energy-dependent xanthoferrin synthesis and uptake system may have evolved in Xcc as a mechanism to take up iron under iron-depleted conditions, such as in the host environment.

This study is also important from the disease perspective, as targeting of the iron uptake system in these bacteria could help to prevent disease development in the near future. Further, a thorough understanding of iron uptake systems in different bacteria may aid in the development of novel strategies to control various animal and plant diseases, which are mainly dependent on the iron uptake ability of pathogens.

EXPERIMENTAL PROCEDURES

Bacterial strains, plasmids and culture conditions

The bacterial strains and plasmids used in this study are listed in Table S2. Xcc 8004 strains were grown at 28 °C in PS medium (Tsuchia *et al.*, 1982) at 200 rpm (New Brunswick Scientific, Innova 43, Edison, NJ, USA). The concentrations of antibiotics used were as follows: rifampicin (Rif), 50 μg/mL; kanamycin (Kan), 50 μg/mL; tetracycline (Tet), 5 μg/mL; gentamycin (Gent), 5 μg/mL; ampicillin (Amp), 50 μg/mL. We used an iron chelator, DP (Fluka Analytical, Steinheim, Westphalia, Germany), to create the low-iron conditions.

Molecular biology and microbiology techniques

All standard molecular biology techniques, including plasmid isolations, genomic DNA isolations, gel extractions and PCR purifications, were performed as described by Sambrook *et al.* (1989) or using kits provided by Qiagen Inc., (Valencia, CA, USA). PCR amplifications were carried out with high-fidelity accu taq polymerase (Sigma-Aldrich, St. Louis, MO, USA), KAPA HiFi HotStart DNA Polymerase (Kappa Biosystems Inc., Wilmington, MA, USA) and Taq polymerase (Thermo Fisher Scientific, Waltham, MA, USA) according to the user manuals provided by the manufacturers. Restriction digestions and ligations were performed with enzymes provided by New England Biolabs (Ipswich, MA, USA) according to the user

manual provided by the manufacturer. Transformations were performed by electroporation, the heat shock method or conjugation. The primers used in this study are listed in Table S4 (see Supporting Information).

Generation of Δ*xssA* and Δ*xsuA* deletion mutants in the wild-type Xcc 8004 background

In-frame marker-free deletion strains were prepared as described previously by Schäfer *et al.* (1994) with a few modifications. The chromosomal deletion of the *xssA* and *xsuA* genes in the Xcc 8004 background was obtained by allelic exchange and homologous recombination using the suicide vector pK18mobsacB harbouring 5′ and 3′ flanking regions of the gene to be deleted. The 5′ flanking regions of Δ*xssA* and Δ*xsuA* were amplified with the primers (listed in Table S4) SCPsidelxc1F & SCPsidelxc2R and SCPxsuAdel 1F & SCPxsuA1R, respectively, whereas the 3′ flanking regions were amplified with the primers SCPsidelxc2F & SCPsidelxc2R and SCPxsuAdel2F & SCPxsuAdel2R, respectively. The 5′ and 3′ flanking PCR products were digested with a common restriction enzyme (*Xba*I) and ligated. The ligation product was PCR amplified with end primers to select the deletion construct. The PCR products and pK18mobsacB were then digested with appropriate restriction enzymes (*Bam*H1 & *Hind*III for the deletion of *xssA* and *Eco*RI & *Hind*III for the deletion of *xsuA*), ligated and transformed in *E. coli* DH5α cells. Appropriate clones were selected on nalidixic acid and kanamycin-containing Luria–Bertani (LB) agar plates and confirmed by nucleotide sequencing. pK18mobsacB carrying deletion constructs (Table S2) was transformed into the wild-type Xcc 8004 strain by electroporation, and transformants with single crossover were selected on nutrient agar (NA) plates containing rifampicin and kanamycin. Colonies were passaged in antibiotic-free nutrient broth medium for the second recombination to occur for the removal of the plasmid background, and eventually selected on PSA containing rifampicin and 5% sucrose. Colonies growing on PSA, but not on NA with kanamycin, were confirmed by the sequencing of PCR products amplified using the outward primers (Table S4): SCP54F Sid del out 2 & SCP54R Sid del out 2 and SCPxsuA del out F and SCPxsuAdel2R for deletion in the *xssA* and *xsuA* genes, respectively. For complementation, the cosmid clone with a 38.2-kb genomic insert of Xoo containing the entire *xss* cluster (pAP15) (Table S2; Pandey and Sonti, 2010) was mobilized in the Δ*xssA* and Δ*xsuA* background by biparental mating with *E. coli* strain S17′-1 harbouring pAP15.

Generation of chromosomal promoter fusions to GUS

Chromosomal fusions of the promoter of the *xss* gene cluster with GUS were created using the suicidal plasmid pVO155 containing the promoterless *gusA* gene, as described previously (Oke and Long, 1999; Pandey and Sonti, 2010) with a few modifications. Briefly, a 971-bp sequence (upstream of the *xsuA* gene) containing the putative promoter of the *xss* gene cluster (Fig. S2; Table S2) was amplified with SCP_sid_prom F & SCP_sid_prom R primers (listed in Table S4) and cloned at the *Hind*III-*Xba*I site of the promoterless suicidal plasmid pVO155. The GUS reporter construct was mobilized from *E. coli* DH5α to *E. coli* S17-1 by triparental mating, and subsequently introduced into wild-type Xcc 8004 by biparental mating with the S17′-1 construct. Insertion of the *gus* reporter cassette was confirmed by PCR amplification and sequencing with primers specific for *gusA* and the neighbouring flanking sequence (data not shown).

Growth under low-iron conditions

We used different concentrations of DP (75, 100 and 150 μM) to create low-iron conditions in PS medium in order to identify the conditions inducing siderophore production without affecting the growth of different Xcc strains, and also to identify the low-iron conditions in which the siderophore-deficient mutants exhibit growth deficiency (Figs 2 and S10, see Supporting Information). We found that 75 μM DP induced siderophore production in the wild-type Xcc 8004 strain, but did not cause significant growth defects in the wild-type or the Δ*xsuA* and Δ*xssA* mutants (Fig. S10B). To induce siderophore production and purification from liquid PS medium, we used 100 μM DP. We found that 100 μM DP did not cause severe growth deficiency in the Δ*xsuA* and Δ*xssA* mutants compared with the wild-type Xcc 8004 strain (Fig. S10C). At 150 μM DP, we observed that the Δ*xsuA* and Δ*xssA* mutants exhibited growth deficiency which could be rescued by supplementation of either iron or purified siderophores. Therefore, for growth assay under low-iron conditions, we used 150 μM DP in this study (Fig. 2).

CAS plate assays for the assessment of siderophore production

CAS agar plate assays for the assessment of siderophore production were performed as described previously (Schwyn and Neilands, 1987) with a few modifications (Chatterjee and Sonti, 2002). *Xanthomonas* grew quite slowly on minimal medium MM9; therefore, we used rich PSA medium supplemented with 75 μM DP to create low-iron conditions. The different Xcc strains were spotted onto the CAS agar plate and incubated at 28 °C.

Purification and quantification of xanthoferrin

Primary cultures of different Xcc strains were grown up to 1.0×10^9 cells/mL in PS broth with the respective antibiotics (see Table S2); 0.3% of inoculum was transferred to 500 mL of PS medium supplemented with 100 μM DP and grown to an optical density at 600 nm (OD_{600}) of unity at 28 °C in a shaking incubator at 200 rpm (New Brunswick Scientific). The cultures were centrifuged at 13201 *g* for 1 h. The supernatants from different cultures were collected and further filtered through a 0.22-μm membrane to remove the remaining cells. Initially, the siderophore was isolated from cell-free supernatants using Amberlite XAD-16 resin columns, as described by Wright (2010) with a few modifications. Briefly, the different cell-free supernatants were acidified up to pH 2 with concentrated HCl and allowed to pass through the prepared XAD-16 resin column (2.4×30 cm^2). Elution was performed with methanol and the flow-through was collected into 100 fractions. Each fraction was tested for siderophores on CAS agar plates supplemented with 75 μM DP. As a negative control, empty buffer eluate from the column run was spotted onto a PSA–CAS + 75 μM DP plate to detect any cross-contaminating CAS-reactive agent during the separation of xanthoferrin (Fig. S11, see Supporting Information). Further, we processed the samples with an Agilent 1100series HPLC system (Agilent, Santa Clara, CA, USA). The data were recorded and analysed using chemstation software (Agilent 1100). We compared the chromatogram of xanthoferrin with the chromatogram of standard purified vibrioferrin (a kind gift from M. J. Fujita). The estimation of siderophore production was performed as described previously (Amin *et al.*, 2009) with a few modifications. The xanthoferrin production by

different Xcc strains was estimated by comparing the peak area at a particular retention time with standard curves generated from a known concentration of pure standard vibrioferrin.

Iron uptake assay

We performed the iron uptake assays using radiolabelled iron as described previously (Ardon *et al.*, 1997; Velayudhan *et al.*, 2000) with a few modifications. Primary cultures of different Xcc strains were grown to 1.0×10^9 cells/mL in rich PS medium with the respective antibiotics (Table S2); 0.3% of inoculum was transferred to fresh PS medium containing 150 μM DP and the antibiotic required to maintain cosmids, and grown to the late stationary phase. Further bacterial cells were harvested and washed twice in 50 mM sodium phosphate buffer (pH 7.4). Bacterial pellets were resuspended in 50 mM sodium phosphate buffer and subsequently diluted with chelex-100 (Sigma, St. Louis, MO, USA)-treated PS to an OD_{600} of 1.0 and incubated at 28 °C for 5 min. The Fe^{3+} uptake was initiated by the addition of 0.4 μM of $^{55}FeCl_3$ (specific activity of 10.18 mCi/mg; American Radiolabeled Chemicals, Inc., St. Louis, MO, USA). For the uptake assay of the Fe^{3+}–xanthoferrin complex, the uptake was initiated after combining vibrioferrin (7.6 mM stock) and $^{55}FeCl_3$ in a 1 : 1 ratio. Uptake was stopped at different time points by layering onto di-butyl phthalate and di-octyl phthalate (1 : 1) solution. Immediately, the cultures were centrifuged at 17968 g for 2 min; eventually, the pellets were resuspended in 100 μL of 1% (v/v) Triton X-100. The suspensions were transferred to 5 mL of scintillation cocktail and counted in the ^3H channel of a scintillation counter (Perkin-Elmer, Waltham, MA, USA, Liquid Scintillation Analyzer, Tri-Carb 2910 TR, USA). As a control, iron uptake was performed in the presence of carbonyl cyanide *p*-trifluoromethoxy phenylhydrazone (FCCP; 50 μM), a proton motive force uncoupler. There was no significant increase in the incorporation of radiolabelled iron in the presence of FCCP, indicating that iron uptake is an energy-dependent process (data not shown).

Streptonigrin sensitivity assay

To assess intracellular iron content, we performed streptonigrin sensitivity assay as described previously (Wilson *et al.*, 1998) with a few modifications. Briefly, overnight-grown cultures of different Xcc strains were harvested by centrifugation at 3300 g for 5 min. Pellets were resuspended in fresh PS medium at $OD_{600} = 0.6$; 2% of inoculum was transferred to 4 mL of fresh PS medium with and without streptonigrin (Sigma-Aldrich) and sodium citrate in six-well plates. The plates were incubated in a static incubator at 28 °C. Absorbance at 600 nm was measured after 16 and 40 h of incubation. The percentage survival was calculated by comparing the bacterial growth in streptonigrin relative to that in rich PS medium. This assay was also performed on a PSA plate containing streptonigrin and sodium citrate by spotting serial dilutions of cell-normalized bacterial cultures.

Estimation of intracellular iron level

The intracellular iron content was estimated using atomic absorption spectrophotometry as described previously (Velayudhan *et al.*, 2000) with a few modifications. Different Xcc strains were grown to stationary phase culture in rich PS, PS with 150 μM $FeSO_4$ (Fe-replete) and PS with 100 μM DP (Fe-restricted) media. Cells were harvested by centrifugation, followed by washing twice with phosphate-buffered saline (50 mM PBS, pH 7.4). Pellets were lyophilized and their dry weights were determined. A further equal amount of lyophilized cells was solubilized in 30% HNO_3 at 80 °C overnight and subsequently diluted 10-fold with sterile milliQ water. The iron content was determined using ICP-OES (JY 2000 sequential ICP-OES spectrometer, Jobin Yvon, Horiba, France).

GUS reporter assays

The GUS reporter strain was grown in rich PS medium with the required antibiotics at 28 °C and 200 rpm overnight; 0.2% of primary inoculum was transferred to rich PS, PS with 100 μM $FeSO_4$ (Fe-replete), PS with 100 μM DP (Fe-restricted) and PS with 100 μM DP + 100 μM $FeSO_4$ ($FeSO_4$ supplementation to Fe-restricted) media. The absorbance at 600 nm and GUS expression were measured at regular time intervals. GUS expression assays were performed as described previously (Jefferson *et al.*, 1987) with a few modifications. Briefly, cells were harvested from 1 mL of culture and washed with sterile milliQ water. Pellets were resuspended in 250 μL extraction buffer [50 mM sodium dihydrogen phosphate (pH 7.0), 10 mM ethylenediaminetetraacetic acid (EDTA), 10 mM β-mercaptoethanol, 0.1% Triton X-100 and 0.1% sodium lauryl sarcosine] with added 1 mM MUG (4-methylumbelliferyl β-D-glucuronide) and incubated at 37 °C. After a definite time interval, reactions were terminated by the addition of 675 μL of 0.2 M Na_2CO_3 into 75 μL of reaction mixture. Fluorescence was measured with 4-methylumbelliferone (4-MU; Sigma) as standard at an excitation wavelength of 365 nm and emission wavelength of 455 nm. GUS activity was presented as nanomoles of 4-MU produced per minute.

In planta GUS expression assay

The GUS reporter strain was grown to 1.0×10^9 cells/mL in the presence or absence of 100 μM DP or 100 μM $FeSO_4$. Cells were harvested, washed with sterile milliQ water and infiltrated into cabbage leaves (Indian Super Hybrid variety) with and without 100 μM DP or 100 μM $FeSO_4$. The leaves were harvested at 0, 2, 4, 6 and 8 dpi and crushed in 1 mL of extraction buffer [50 mM sodium dihydrogen phosphate (pH 7.0), 0.1% Triton X-100, 10 mM EDTA, 0.1% sodium lauryl sarcosine and 10 mM β-mercaptoethanol] without substrate. Subsequently, 250 μL of extraction buffer with 1 mM MUG substrate was added to the plant extract and incubated at 37 °C. Reactions were stopped by the addition of 675 μL of 0.2 M Na_2CO_3 into 75 μL of reaction mixture. Fluorescence was measured with 4-MU (Sigma) as standard at an excitation wavelength of 365 nm and emission wavelength of 455 nm. GUS activity was expressed as nanomoles of MU produced per minute per square centimetre of leaf area.

Histochemical staining

Thirty-day-old cabbage leaves (Indian Super Hybrid variety) were infiltrated with GUS reporter strains in the presence or absence of 100 μM DP or 100 μM $FeSO_4$. At 5 dpi, the leaves were stained with 1 mM X-Gluc in GUS assay buffer [50 mM sodium dihydrogen phosphate (pH 7.0), 10 mM EDTA, 0.1% sodium lauryl sarcosine, 0.1% Triton X-100 and 10 mM β-mercaptoethanol] to determine β-D-glucuronidase activity. A vacuum was applied for 1 h to facilitate X-Gluc penetration into the leaves and then

incubated at 37 °C for 2 h. Subsequently, chlorophyll was removed from the leaves by incubation in absolute alcohol for 72 h at 37 °C, and then observed under a compound microscope. The experiment was performed with a minimum of five infiltrated leaves for each strain and repeated three times.

Assay for Fe^{3+} reductase activity

The Fe^{3+} reductase activity of Xcc strains was measured using ferrozine (Sigma-Aldrich), a chromogenic Fe^{2+} chelator, as described previously (Deneer *et al.*, 1995; Velayudhan *et al.*, 2000; Worst *et al.*, 1998) with slight modifications. Briefly, 1 mM ferrozine and 100 μM $FeCl_3$ were added to different Xcc strains, grown to a density of 1.0×10^6 cells/mL and incubated at 28 °C. Cell-free PS medium was incubated under the same conditions as a blank; 1-mL aliquots were taken at each time interval and centrifuged at 17968 g for 2 min. The absorbance of the magenta-coloured Fe^{2+}–ferrozine complex in the supernatant was measured at 562 nm.

Virulence assays on cabbage plants

Virulence assay was conducted by inoculation of Xcc strains onto 30-day-old Indian cabbage (Indian Super Hybrid variety) using the scissor-clipping method. In brief, different Xcc strains were grown to a density of 1.0×10^9 cells/mL in PS medium with the required antibiotics. Cells were pelleted down at 3300 g for 5 min and resuspended in sterile milliQ water. Sterile scissors were dipped in bacterial cultures and cabbage leaves were gently incised at the apex. The lesion length, number of colony-forming units (CFU) and migration of bacteria inside host leaves were recorded. A plant inoculated with sterile milliQ water was used as a control (Robinson and Callow, 1986).

Exogenous iron supplementation and bacterial growth assay in cabbage leaves

Exogenous iron supplementation and bacterial growth assays in detached leaves were performed as described previously (Chatterjee and Sonti, 2002) with a few modifications. Leaves, together with the petiole, of 30-day-old cabbage plants were cut with sterile scissors and dipped in 250-mL beakers (four to six leaves per beaker) containing 100 mL of 1.0 μg/mL of BAP with or without 50 μM $FeCl_3$ (Standard Reagents, Hyderabad, India) in sterile milliQ water. The addition of BAP, a first-generation synthetic cytokinin, helped to maintain the detached cabbage leaves in a fresh condition. In a control experiment, we added red-coloured safranin dye to a beaker containing BAP to determine the conductance of water in the leaves. After overnight incubation, the spread of red colour into the leaves indicated water conductance (Fig. S5B). The leaves were clip inoculated with cultures of different Xcc strains at a density of 1.0×10^9 cells/mL. Bacterial growth was determined by the number of CFU obtained after crushing the surface-sterilized 1-cm^2 leaf area surrounding the inoculation site, followed by dilution plating.

ACKNOWLEDGEMENTS

We are grateful to Dr Masaki J. Fujita (Hokkaido University, Japan) for providing the pure vibrioferrin standard. S.S.P. and R.R were recipients of Senior Research Fellowships from the Council of Scientific and Industrial Research (CSIR), India. This study was supported by funding to S.C. from the Department of Biotechnology (DBT), Council of Scientific & Industrial Research - Human Resource Development Group (CSIR-HRDG), Department of Science and Technology - Science & Engineering Research Board (DST-SERB), Government of India and core funding from Centre for DNA Fingerprinting and Diagnostics (CDFD), Hyderabad, India.

REFERENCES

Amin, S.A., Green, D.H., Küpper, F.C. and Carrano, C.J. (2009) Vibrioferrin, an unusual marine siderophore: iron binding, photochemistry, and biological implications. *Inorg. Chem.* **48**, 11 451–11 458.

Andrews, S.C., Robinson, A.K. and Rodríguez-Quiñones, F. (2003) Bacterial iron homeostasis. *FEMS Microbiol. Rev.* **27**, 215–237.

Angerer, A., Gaisser, S. and Braun, V. (1990) Nucleotide sequences of the sfuA, sjiiB, and sfiC genes of *Serratia marcestens* suggest a periplasmic-binding protein-dependent iron transport mechanism. *J. Bacteriol.* **172**, 572–578.

Ardon, O., Weizman, H., Libman, J., Shanzer, A., Chen, Y. and Hadar, Y. (1997) Iron uptake in *Ustilago maydis*: studies with fluorescent ferrichrome analogues. *Microbiology*, **143**, 3625–3631.

Bearden, S.W., Fetherston, J.D. and Perry, R.D. (1997) Genetic organization of the yersiniabactin biosynthetic region and construction of avirulent mutants in *Yersinia pestis*. *Infect. Immun.* **65**, 1659–1668.

Bhatt, G. and Denny, T.P. (2004) *Ralstonia solanacearum* iron scavenging by the siderophore staphyloferrin B is controlled by PhcA, the global virulence regulator. *J. Bacteriol.* **186**, 7896–7904.

Braun, V. and Hantke, K. (2013) The tricky ways bacteria cope with iron limitation. In Iron Uptake in Bacteria with Emphasis on E. coli and Pseudomonas. (Chakraborty, R., Braun, V., Hantke, K., and Cornelis, P., eds), pp. 31–66. Netherlands: Springer.

Bull, C.T., Carnegie, S.R. and Loper, E.J. (1996) Pathogenicity of mutants of *Erwinia carotovora* subsp. *carotovora* deficient in aerobactin and catecholate siderophore production. *Mol. Plant Pathol.* **86**, 260–266.

Cartron, M.L., Maddocks, S., Gillingham, P., Craven, C.J. and Andrews, S.C. (2006) Feo – transport of ferrous iron into bacteria. *BioMetals*, **19**, 143–157.

Cassat, J.E. and Skaar, E.P. (2013) Iron in infection and immunity. *Cell Host Microbe*, **13**, 509–519.

Chatterjee, S. and Sonti, R.V. (2002) rpfF mutants of *Xanthomonas oryzae* pv. *oryzae* are deficient for virulence and growth under low iron conditions. *Mol. Plant–Microbe. Interact.* **15**, 463–471.

Cohen, M.S., Chai, Y., Britigan, B.E., McKenna, W., Adams, J., Svendsen, T., Bean, K., Hassett, D.J. and Sparling, P.F. (1987) Role of extracellular iron in the action of the quinone antibiotic streptonigrin: mechanisms of killing and resistance of *Neisseria gonorrhoeae*. *Antimicrob. Agents Chemother.* **31**, 1507–1513.

Dale, S.E., Doherty-Kirby, A., Lajoie, G., Heinrichs, D.E., Al, D.E.T. and Mmun, I.N.I. (2004) Role of siderophore biosynthesis in virulence of Staphylococcus aureus: identification and characterization of genes involved in production of a siderophore. *Infect. Immun.* **72**, 29–37.

Dellagi, A., Brisset, M.N., Paulin, J.P. and Expert, D. (1998) Dual role of desferrioxamine in *Erwinia amylovora* pathogenicity. *Mol. Plant–Microbe. Interact.* **11**, 734–742.

Deneer, H.G., Healey, V. and Boychuk, I. (1995) Reduction of exogenous ferric iron by a surface-associated ferric reductase of *Listeria* spp. *Microbiology*, **141**, 1985–1992.

Enard, C., Diolez, A. and Expert, D. (1988) Systemic virulence of *Erwinia chrysanthemi* 3937 requires a functional iron assimilation system. *J. Bacteriol.* **170**, 2419–2426.

Etchegaray, A., Silva-Stenico, M.E., Moon, D.H. and Tsai, S.M. (2004) In silico analysis of nonribosomal peptide synthetases of *Xanthomonas axonopodis* pv. *citri*: identification of putative siderophore and lipopeptide biosynthetic genes. *Microbiol. Res.* **159**, 425–437.

Expert, D., Enard, C. and Masclaux, C. (1996) The role of iron in plant host–pathogen interactions. *Trends Microbiol.* **4**, 232–237.

Expert, D., Franza, T. and Dellagi, A. (2012) Molecular aspects of iron metabolism in pathogenic and symbiotic plant–microbe associations. In SpringerBriefs in Biometals. (Expert, D. and O Brian, M.R., eds), pp. 7–39. London WC1X 8HB, UK: Springer.

Faraldo-Gómez, J.D. and Sansom, M.S.P. (2003) Acquisition of siderophores in gram-negative bacteria. *Nat. Rev. Mol. Cell Biol.* **4**, 105–116.

Ferguson, A.D. and Deisenhofer, J. (2004) Metal import through microbial membranes. *Cell*, **116**, 15–24.

Franza, T., Mahé, B. and Expert, D. (2005) *Erwinia chrysanthemi* requires a second iron transport route dependent on the siderophore achromobactin for extracellular growth and plant infection. *Mol. Microbiol.* **55**, 261–275.

Fujita, M.J., Kimura, N., Sakai, A., Ichikawa, Y., Hanyu, T. and Otsuka, M. (2011) Cloning and heterologous expression of the vibrioferrin biosynthetic gene cluster from a marine metagenomic library. *Biosci. Biotechnol. Biochem.* **75**, 2283–2287.

Guerinot, M.L. (1994) Microbial iron transport. *Annu. Rev. Microbiol.* **48**, 743–772.

Henderson, D.P. and Payne, S.M. (1994) Vibrio-cholerae iron transport-systems – roles of heme and siderophore iron transport in virulence and identification of a gene associated with multiple iron transport-systems. *Infect. Immun.* **62**, 5120–5125.

Jefferson, R.A., Kavanagh, T.A. and Bevan, M.W. (1987) GUS fusions: beta-glucuronidase as a sensitive and versatile gene fusion marker in higher plants. *Embo J.* **6**, 3901–3907.

Jones, A.M. and Wildermuth, M.C. (2011) The phytopathogen *Pseudomonas syringae* pv. *tomato* DC3000 has three high-affinity iron-scavenging systems functional under iron limitation conditions but dispensable for pathogenesis. *J. Bacteriol.* **193**, 2767–2775.

Jones, C.M. and Niederweis, M. (2010) Role of porins in iron uptake by *Mycobacterium smegmatis*. *J. Bacteriol.* **192**, 6411–6417.

Kammler, M., Schön, C. and Hantke, K. (1993) Characterization of the ferrous iron uptake system of *Escherichia coli*. *J. Bacteriol.* **175**, 6212–6219.

Krewulak, K.D. and Vogel, H.J. (2008) Structural biology of bacterial iron uptake. *Biochim. Biophys. Acta*, **1778**, 1781–1804.

Larsen, R.A., Thomas, M.G. and Postle, K. (1999) Proton motive force, ExbB and ligand-bound FepA drive conformational changes in TonB. *Mol. Microbiol.* **31**, 1809–1824.

Lawlor, M.S., O'Connor, C. and Miller, V.L. (2007) Yersiniabactin is a virulence factor for *Klebsiella pneumoniae* during pulmonary infection. *Infect. Immun.* **75**, 1463–1472.

Lee, B.M., Park, Y.J., Park, D.S, Kang, H.W., Kim, J.G., Song, E.S., Park, I.C., Yoon, U.H., Hahn, J.H., Koo, B.S., Lee, G.B., Kim, H., Park, H.S., Yoon, K.O., Kim, J.H., Jung, C.H., Koh, N.H., Seo, J.S. and Go, S.J. (2005) The genome sequence of *Xanthomonas oryzae* pathovar *oryzae* KACC10331, the bacterial blight pathogen of rice. *Nucleic Acids Res.* **33**, 577–586.

Meyer, J.M., Neely, A., Stintzi, A., Georges, C. and Holder, I.A. (1996) Pyoverdin is essential for virulence of *Pseudomonas aeruginosa*. *Infect. Immun.* **64**, 518–523.

Miethke, M. and Marahiel, M.A. (2007) Siderophore-based iron acquisition and pathogen control. *Microbiol. Mol. Biol. Rev.* **71**, 413–451.

Neilands, J.B. (1981) Microbial iron compounds. *Annu. Rev. Biochem.* **50**, 715–731.

Noinaj, N., Guillier, M., Barnard, T.J. and Buchanan, S.K. (2010) TonB-dependent transporters: regulation, structure, and function. *Annu. Rev. Microbiol.* **64**, 43–60.

Oke, V. and Long, S.R. (1999) Bacterial genes induced within the nodule during the Rhizobium ± legume symbiosis. *Mol. Microbiol.* **32**, 837–849.

Pandey, A. and Sonti, R.V. (2010) Role of the FeoB protein and siderophore in promoting virulence of *Xanthomonas oryzae* pv. *oryzae* on rice. *J. Bacteriol.* **192**, 3187–3203.

Qian, W., Jia, Y., Ren, S.X., He, Y.Q., Feng, J.X., Lu, L.F., Sun, Q., Ying, G., Tang, D.J., Tang, H., Wu, W., Hao, P., Wang, L., Jiang, B.L., Zeng, S., Gu, W.Y., Lu, G., Rong, L., Tian, Y., Yao, Z., Fu, G., Chen, B., Fang, R., Qiang, B., Chen, Z., Zhao, G.P., Tang, J.L. and He, C. (2005) Comparative and functional genomic analyses of the pathogenicity of phytopathogen. *Genome Res.* **15**, 757–767.

Rai, R., Javvadi, S. and Chatterjee, S. (2015) Cell–cell signaling promotes ferric iron uptake in *Xanthomonas oryzae* pv. *oryzicola* that contributes to its virulence and growth inside rice. *Mol. Microbiol.* **96**, 789–801.

Robinson, J.N. and Callow, J.A. (1986) Multiplication and spread of pathovars of *Xanthomonas campestris* in host and non-host plants. *Plant Pathol.* **35**, 169–177.

Rondon, M.R., Ballering, K.S. and Thomas, M.G. (2004) Identification and analysis of a siderophore biosynthetic gene cluster from *Agrobacterium tumefaciens* C58. *Microbiology*, **150**, 3857–3866.

Ryan, R.P., Vorhölter, F.J., Potnis, N., Jones, J.B., Van Sluys, M.A., Bogdanove, A.J. and Dow, J.M. (2011) Pathogenomics of *Xanthomonas*: understanding bacterium–plant interactions. *Nat. Rev. Microbiol.* **9**, 344–355.

Sambrook, J., Fritsch, E.F. and Maniatis, T.A. (1989) Molecular Cloning: A Laboratory Manua 2nd ed., Cold Spring Harbor, NY, U.S.A:Cold Spring Harbor Laboratory Press.

Schäfer, A., Tauch, A., Jäger, W., Kalinowski, J., Thierbach, G. and Pühler, A. (1994) Small mobilizable multi-purpose cloning vectors derived from the *Escherichia coli* plasmids pK18 and pK19: selection of defined deletions in the chromosome of *Corynebacterium glutamicum*. *Gene*, **145**, 69–73.

Schaible, U.E. and Kaufmann, S.H.E. (2004) Iron and microbial infection. *Nat. Rev. Microbiol.* **2**, 946–953.

Schmitt, M.P. (1997) Utilization of host iron sources by *Corynebacterium diphtheriae*: identification of a gene whose product is homologous to eukaryotic heme oxygenases and is required for acquisition of iron from heme and hemoglobin. *J. Bacteriol.* **179**, 838–845.

Schröder, I., Johnson, E. and de Vries, S. (2003) Microbial ferric iron reductases. *FEMS Microbiol. Rev.* **27**, 427–447.

Schwyn, B. and Neilands, J.B. (1987) Universal chemical assay for the detection and determination of siderophores. *Anal. Biochem.* **160**, 47–56.

da Silva, A.C., Ferro, J.A., Reinach, F.C., Farah, C.S., Furlan, L.R., Quaggio, R.B., Monteiro-Vitorello, C.B., Van Sluys, M.A., Almeida, N.F., Alves, L.M., do Amaral, A.M., Bertolini, M.C., Camargo, L.E., Camarotte, G., Cannavan, F., Cardozo, J., Chambergo, F., Ciapina, L.P., Cicarelli, R.M., Coutinho, L.L., Cursino-Santos, J.R., El-Dorry, H., Faria, J.B., Ferreira, A.J., Ferreira, R.C., Ferro, M.I., Formighieri, E.F., Franco, M.C., Greggio, C.C., Gruber, A., Katsuyama, A.M., Kishi, L.T., Leite, R.P., Lemos, E.G., Lemos, M.V., Locali, E.C., Machado, M.A., Madeira, A.M., Martinez-Rossi, N.M., Martins, E.C., Meidanis, J., Menck, C.F., Miyaki, C.Y., Moon, D.H., Moreira, L.M., Novo, M.T., Okura, V.K., Oliveira, M.C., Oliveira, V.R., Pereira, H.A., Rossi, A., Sena, J.A., Silva, C., de Souza, R.F., Spinola, L.A., Takita, M.A., Tamura, R.E., Teixeira, E.C., Tezza, R.I., Trindade dos Santos, M., Truffi, D., Tsai, S.M., White, F.F., Setubal, J.C. and Kitajima, J.P. (2002) Comparison of the genomes of two *Xanthomonas* pathogens with differing host specificities. *Nature*, **417**, 459–463.

Tanabe, T., Funahashi, T., Nakao, H., Miyoshi, S., Shinoda, S. and Yamamoto, S. (2003) Identification and characterization of genes required for biosynthesis and transport of the siderophore vibrioferrin in *Vibrio parahaemolyticus*. *J. Bacteriol.*, **185**, 6938–6949.

Tsuchia, K., Mew, T.W. and Wakimoto, S. (1982) Bacteriological and pathological charecteristics of wild types and induced mutants of Xanthomonas campestris pv. oryzae. *Phytopathology*, **72**, 43–46.

Velayudhan, J., Hughes, N.J., McColm, A.A., Bagshaw, J., Clayton, C.L., Andrews, S.C. and Kelly, D.J. (2000) Iron acquisition and virulence in *Helicobacter pylori*: a major role for FeoB, a high-affinity ferrous iron transporter. *Mol. Microbiol.* **37**, 274–286.

Weinberg, E.D. (2009) Iron availability and infection. *Biochim. Biophys. Acta*, **1790**, 600–605.

Wiener, M.C. (2005) TonB-dependent outer membrane transport: going for Baroque? *Curr. Opin. Struct. Biol.* **15**, 394–400.

Wiggerich, H.G. and Pühler, A. (2000) The exbD2 gene as well as the iron-uptake genes tonB, exbB and exbD1 of *Xanthomonas campestris* pv. *campestris* are essential for the induction of a hypersensitive response on pepper (*Capsicum annuum*). *Microbiology*, **146**, 1053–1060.

Wiggerich, H.G., Klauke, B., Köplin, R., Priefer, U.B. and Pühler, A. (1997) Unusual structure of the tonB-exb DNA region of *Xanthomonas campestris* pv. *campestris*: tonB, exbB, and exbD1 are essential for ferric iron uptake, but exbD2 is not. *J. Bacteriol.* **179**, 7103–7110.

Wilson, T.J., Bertrand, N., Tang, J.L., Feng, J.X., Pan, M.Q., Barber, C.E., Dow, J.M. and Daniels, M.J. (1998) The rpfA gene of *Xanthomonas campestris* pathovar *campestris*, which is involved in the regulation of pathogenicity factor production, encodes an aconitase. *Mol. Microbiol.* **28**, 961–970.

Worst, D.J., Gerrits, M.M., Vandenbroucke-Grauls, C.M.J.E. and Kusters, J.G. (1998) *Helicobacter pylori ribBA*-mediated riboflavin production is involved in iron acquisition. *J. Bacteriol.* **180**, 1473–1479.

Wright, W.H. IV (2010) "Isolation and Identification of the Siderophore "Vicibactin" Produced by Rhizobium leguminosarum ATCC 14479." Electronic Theses and Dissertations. Paper 1690. http://dc.etsu.edu/etd/1690

Yeowell, H.N. and White, J.R. (1982) Iron requirement in the bactericidal mechanism of streptonigrin. *Antimicrob Agents Chemother.* **22**, 961–968.

Zimmermann, L., Angerer, A. and Braun, V. (1989) Mechanistically novel iron(III) transport system in *Serratia marcescens*. *J. Bacteriol.* **171**, 238–243.

SUPPORTING INFORMATION

Additional Supporting Information may be found in the online version of this article at the publisher's website:

Fig. S1 Schematic presentation of the *xss* (*Xanthomonas s*iderophore *s*ynthesis) gene cluster of *Xanthomonas campestris* pv. *campestris* (Xcc) 8004, *Xanthomonas oryzae* pv. *oryzae* and *Vibrio parahaemolyticus*.

Fig. S2 Genetic organization of the *Xanthomonas campestris* pv. *campestris* (Xcc) 8004 *xss* (*Xanthomonas s*iderophore *s*ynthesis) cluster indicating the location of the deletions in the knockout strains Δ*xssA* and Δ*xsuA*, and pSSP70 insertion in the β-glucuronidase (GUS) reporter strain Xcc 8004 P*xss*::*gusA*.

Fig. S3 Relative quantification of the expression of downstream genes of the *xss* (*Xanthomonas s*iderophore *s*ynthesis) operon in Δ*xssA* and Δ*xsuA* mutants compared with the wild-type *Xanthomonas campestris* pv. *campestris* (Xcc) 8004 strain by real-time quantitative reverse transcription-polymerase chain reaction (qRT-PCR).

Fig. S4 High-performance liquid chromatography (HPLC) chromatograms of purified xanthoferrin from different *Xanthomonas campestris* pv. *campestris* (Xcc) strains.

Fig. S5 Purified vibrioferrin from *Vibrio parahaemolyticus* rescues the growth deficiency of the Δ*xssA* mutant under low-iron conditions.

Fig. S6 Streptonigrin sensitivity assay to assess the intracellular iron content among wild-type *Xanthomonas campestris* pv. *campestris* (Xcc) 8004, Δ*xssA*, Δ*xsuA*, Δ*xssA*/pAP15 and Δ*xsuA*/pAP15 strains grown in peptone–sucrose (PS) medium and iron-replete conditions.

Fig. S7 The *Xanthomonas campestris* pv. *campestris* (Xcc) 8004 P*xss*::*gusA* reporter strain exhibits wild-type Xcc 8004-like phenotypes under low-iron conditions.

Fig. S8 Assay for bacterial migration inside cabbage leaves and control experiment for conductance.

Fig. S9 Ferric reductase assay of wild-type *Xanthomonas campestris* pv. *campestris* (Xcc) 8004, Δ*xssA* and Δ*xsuA* strains.

Fig. S10 The growth of *Xanthomonas campestris* pv. *campestris* (Xcc) 8004 (wild-type), Δ*xssA* and Δ*xsuA* strains in different concentrations of 2,2′-dipyridyl.

Fig. S11 Column buffer control and active fraction of wild-type *Xanthomonas campestris* pv. *campestris* (Xcc) xanthoferrin on peptone–sucrose agar and chromeazurol S (PSA–CAS) plates containing 75 μM 2,2′-dipyridyl.

Table S1 Homology of proteins encoded in the *xss* (*Xanthomonas s*iderophore *s*ynthesis; involved in siderophore biosynthesis, putative export and uptake) gene cluster of *Xanthomonas campestris* pv. *campestris* (Xcc) with those of *Vibrio parahaemolyticus*, and *X. oryzae* pv. *oryzae* (Xoo) KACC103331.

Table S2 List of strains and plasmids used in this study.

Table S3 Generation times of different *Xanthomonas campestris* pv. *campestris* (Xcc) strains.

Table S4 List of the primers used in this study.